Removal of Image Segmentation Boundary Errors Using an N-ary Morphological Operator

Thomas P. Weldon
University of North Carolina at Charlotte
Charlotte, NC, 28223, USA
tpweldon@uncc.edu

Abstract

In difficult image segmentation problems, multidimensional feature vectors from filter banks provide effective classification within homogeneous regions. However, such bandlimited feature vectors often exhibit transitory errors at the boundaries between two regions. At boundaries, the feature vector may make a transition through a region of feature space that is incorrectly assigned to a third class. To remove such errors, an N-ary morphological operator is proposed. The overall effect of the proposed operator resembles an N-ary morphological erosion followed by an N-ary dilation.

1. Introduction

In a variety of difficult image segmentation problems, filter banks are used to generate effective features for segmenting an image into different classes of interest [1]-[6]. These filter outputs are then processed by a classifier to form a segmented image. After forming the segmented image, narrow regions near the boundary between two different classes are occasionally misclassified as a third class. This third "false class" typically appears as a narrow strip of misclassified pixels at the boundary.

These narrow misclassified regions can occur when the trajectory of the feature vector makes a transition through feature space at the boundary. As the feature vector changes, it can pass through intermediate feature-space regions assigned to a third class unrelated to the two original classes forming the boundary. Such misclassified regions incidentally appear to be present in the results of prior investigators including Fig. 11 of Jain et al. [1], Fig. 7 of Unser [2], and Fig. 9 of Lu et al. [3].

A two-step hybrid "N-ary" postprocessing operation is proposed to remove these narrow misclassified regions. In the first step, pixels in regions whose neighborhood consists entirely of one texture class are left unchanged; otherwise, the pixel value is set to zero to indicate it is no longer assigned to any class. The neighborhood size is chosen to be proportional to spatial extent of filter-channel response. This first step resembles a morphological erosion operation. In the second step, the classified regions are propagated back into the unassigned regions based on the most common class within 8-neighborhoods. This second step resembles a morphological dilation operation. The combined effect of these two steps is effective in removing the narrow misclassified strips at boundaries between regions.

In the following, details of the proposed method are developed. Then experimental results are presented showing the efficacy of the proposed method.

2. Approach

Before describing the proposed method, a one-dimensional example will be used to describe the underlying problem. In this example, optimal classification thresholds are first calculated for three Gaussian-distributed classes. Then, a step boundary is blurred by a spatial Gaussian filtering operation to simulate the effects of a Gabor-filtered feature. Finally, it is shown that an inevitable band of misclassified pixels results near the boundary, because of the band-limited spatial filtering. A solution to this problem is proposed in the following section.

To illustrate the transient misclassifications that can occur at region boundaries, consider the situation in Fig. 1, with three probability density functions corresponding to the output of a single filter channel for three different classes. It is straightforward to compute optimum thresholds, assuming equal *a priori* likelihood of the three classes [10]. For the example of Fig. 1, the optimal thresholds would be at gray-levels 48 and 165 (other solutions do not contribute materially to the present example). Then, gray-level amplitudes from 0 to 48 are classified as class 1, from 48 to 165 are classified as class 2, and above 165 is classified as class 3.

Next, consider the one-dimensional version of a step boundary between class 1 and class 3 as illustrated by the dashed blue step in Fig. 2. Nominally, this boundary would change from the mean output for class 1, μ_1=30, to the mean of class 3, μ_3=210. However, the step

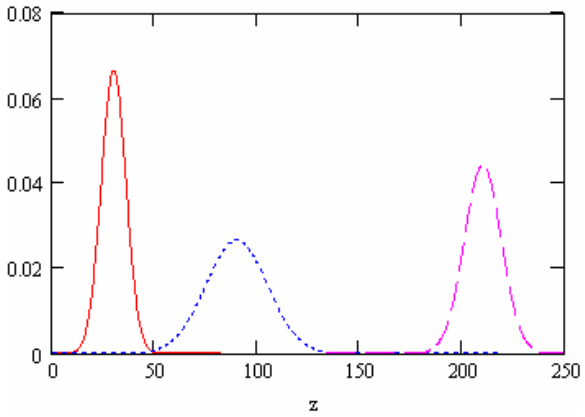

Figure 1. Three Gaussian probability density functions corresponding to filter output features for three different classes: class 1 solid red pdf with μ_1=30, σ_1=6; class 2 dotted blue pdf with μ_2=90, σ_2=15; class 3 dashed magenta pdf with μ_3 = 210, σ_3=9. The optimum classification thresholds for these three pdfs would be at gray-levels 48 and 165.

response at the filter channel output is necessarily smoothed by the filter's limited bandwidth.

To illustrate the response of a bandlimited channel, the step boundary is passed through a lowpass Gaussian filter with spatial-domain standard deviation σ_x=2.5. The resulting smoothed boundary is shown as the red solid curve in Fig 2. The two optimum classification thresholds from Fig. 1 are shown as the horizontal dashed lines in Fig 2. The classifier then makes a correct assignment of class 1 for points more than 3 units to the left of the step, and makes a correct assignment of class 3 for points more than 2 units to the right of the step. However, points in the central region from -3 to +2 units relative to the underlying step are incorrectly classified as class 2. Other bandlimited filters would exhibit a similar misclassification in the transition region. This problem of incorrect classification at region boundaries becomes considerably more complicated in the multi-dimensional case of a multi-channel filter bank and is beyond the scope of the present work.

In practice, these misclassifications near boundaries seem to occur more frequently when the number of filter channels or feature vectors is less than or equal to the number of classes being segmented. This relationship is thought to be some sort of topological dependency between the dimensionality of the classifier and the number of classes. For one-dimensional systems, the foregoing boundary misclassification problem does not occur when there are only two classes, but always occurs when there are more than two classes. In the one-dimensional case of Fig. 1, transitions between the outermost classes must always pass through the middle class.

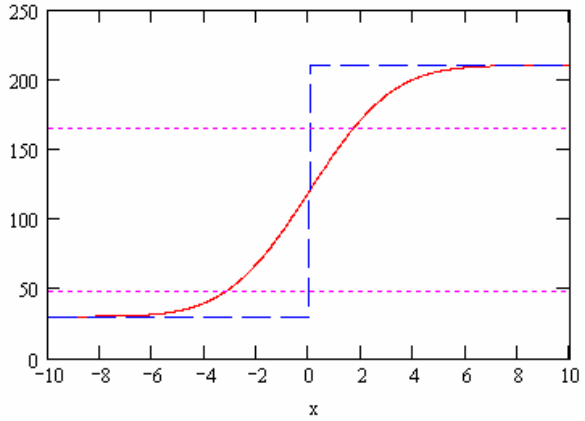

Figure 2. Filtered one-dimensional step boundary, stepping from class 1 (μ_1=30) to class 3 (μ_3=210). Solid red curve is a Gaussian filtered boundary with σ_x=2.5. Dashed blue curve is underlying step boundary. Dotted magenta lines correspond to optimum thresholds from Fig. 1. The region between the two optimum gray-level thresholds of 48 and 165 is misclassified as class 2, with misclassified pixels beginning 3 units to the left and ending 2 units to the right of the actual boundary location.

The example of Fig. 2 is repeated in Fig. 3 in two dimensions. Fig. 3(a) is an image comprised of three Gaussian-distributed random gray levels, and Fig. 3(b) is the resulting image after filtering Fig. 3(a) with a Gaussian lowpass filter with spatial standard deviation of 1.5 pixels.

The dark outer border of Fig 3(b) is comprised of class 1, corresponding to the leftmost pdf in Fig. 1, and the left side of the step boundary in Fig. 2. The bright left-inner rectangular region of Fig. 3(b) is comprised of class 3, corresponding to the rightmost pdf in Fig. 1 and the right side of the step boundary in Fig. 2. The medium gray right-inner rectangular region of Fig. 3(b) is comprised of class 2, corresponding to the central pdf in Fig. 1.

Finally, the classified output image in Fig. 3(c) shows a narrow band of misclassified pixels at the boundary between class 1 (dark gray) and class 3 (white) that are misclassified as class 2 (medium gray). The border is correctly classified as class 1 (dark gray), and the center – left region is correctly classified as class 3 (white). Also, note that the narrow misclassified band does not occur at boundaries between class 1 and class 2, or at boundaries between class 2 and class 3. The misclassified band only occurs at boundaries between class 1 and class 3, since this is the only case where the filtered image gray-level transient response passes through an intermediate gray-level corresponding to a third class as illustrated in Fig. 2.

3. Proposed Operator

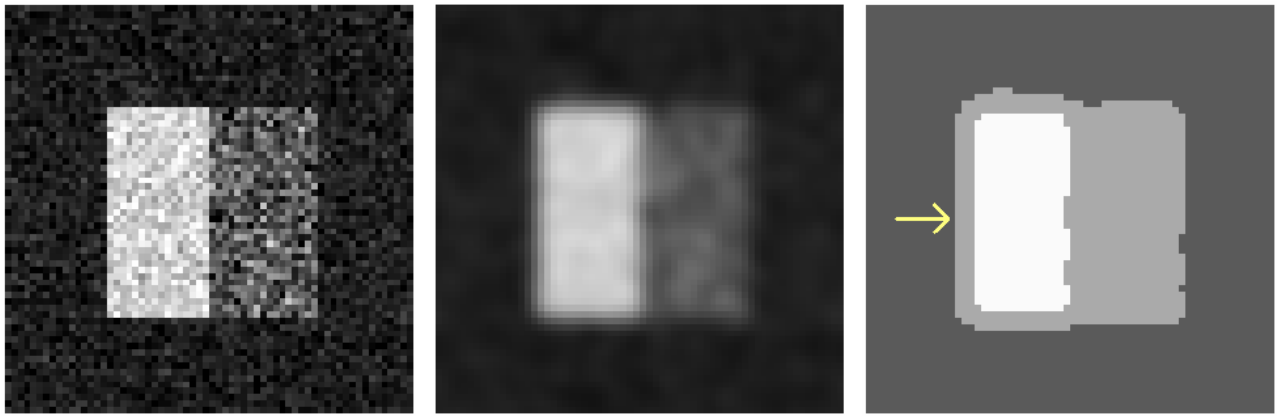

(a) (b) (c)

Figure 3. Two-dimensional example of misclassification. (a) Input 64x64 pixel composite image, outer border is Gaussian noise class 1 with μ_1=30, σ_1=18, right inner rectangle is class 2 with μ_2=90, σ_2=45, and left inner rectangle is class 3 with μ_3 = 210, σ_3=27. (b) Output of Gaussian lowpass filter with spatial standard deviation of σ_x=1.5 pixels. After filtering, class 1 μ_1=30, σ_1=3.3, class 2 μ_2=90, σ_2=8.2, and class 3 μ_3 = 210, σ_3=5.2, analogous to pdfs in Fig. 1. (c) Segmentation using optimal thresholds of 47 and 163, with the yellow arrow pointing at the narrow band of medium gray pixels misclassified as class 2 at the boundary between class1 and class 3. Note that similar narrow bands of misclassified pixels do not occur at other types of boundaries.

The proposed method for eliminating the narrow misclassified regions proceeds in two steps, beginning with a previously classified image c(x,y), where $c(x,y) \in \{1,2,3,\ldots,N\}$ and N is the number of classes. In the first step, boundary regions are reset to an unclassified state. In the second step, classes are propagated back into the unclassified regions. Details are given below.

In the first step, pixels in the classified image c(x,y) whose neighborhood consists entirely of one class are left unchanged; otherwise, the pixel value is set to zero to indicate that the pixel is no longer assigned to any class. The declassification of these pixels creates a new image $i_{S,0}(x,y)$:

$$i_{S,0}(x,y) = \begin{cases} c(x,y), if\ c(x,y) = c(\alpha,\beta)\ \forall (\alpha,\beta) \in B \\ 0, \quad otherwise \end{cases}$$

where B is a local neighborhood typically chosen in some proportion to the spatial extent of the filter channel impulse responses.

In the second step, classified regions are propagated back iteratively into the unassigned regions. Each unassigned pixel is assigned to the most prevalent class within the 8-neighborhood surrounding the pixel.

$$i_{S,n+1}(x,y) = \begin{cases} i_{S,n}(x,y), & if\ i_{S,n}(x,y) \neq 0 \\ 0, & if\ all\ N_8\ neighbors = 0 \\ l_{\max}, & otherwise \end{cases}$$

where l_{max} is the nonzero pixel value that occurs the greatest number of times in the 8-neighborhood, $i_{S,n}(x,y)$ is the image at iteration n. In the event of a tie in determining l_{max}, the pixel is arbitrarily assigned to one of the prevalent classes (other schemes are possible). Step 2 is repeated until all pixels are non-zero, giving the final segmented image $i_S(x;y)$. This propagation affects only unassigned pixels and ceases when all unassigned pixels have been assigned to one of the N classes.

4. Results

The proposed method is shown in Fig. 4 applied to the results of Fig. 3. Fig. 4(a) shows the misclassified image results from Fig 3(c). Fig. 4(b) shows the output, $i_{S,0}(x,y)$, after the first stage of the proposed processing, with declassified pixels shown in black. Finally, the segmented image after all postprocessing, $i_S(x,y)$, is shown in Fig. 4(c). All transient misclassifications are removed.

The proposed method has also been tested on a wide range of natural and synthetic 256×256 pixel 8-bit gray-scale images. In these images, the average gray scale was

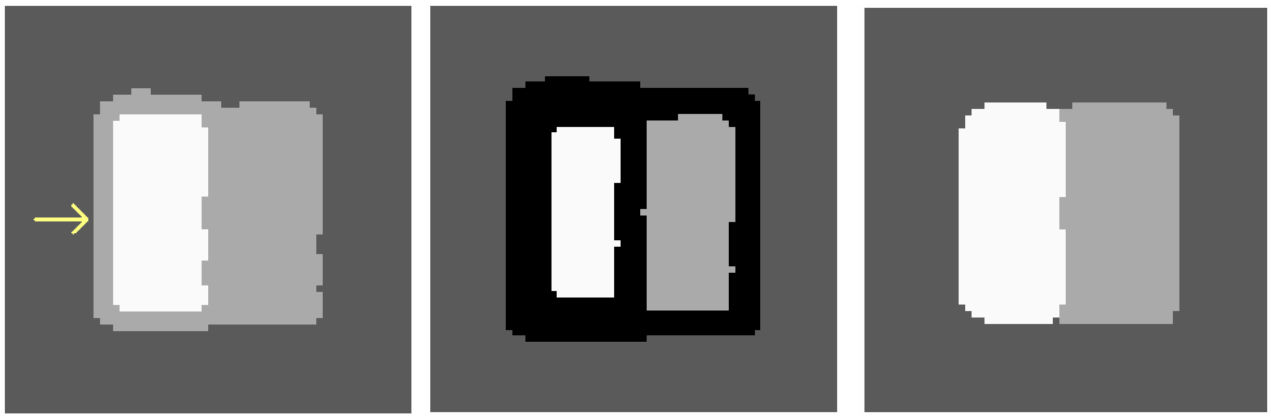

(a) (b) (c)

Figure 4. Proposed postprocessing. (a) Segmented image from Fig. 3(c) showing ring of misclassified pixels at boundary between inner region and outer border. (b) Output $i_{S,0}(x,y)$ after first stage of proposed processing, with declassified pixels shown in black. (c) Final output after final stage of postprocessing, showing classified regions propagated back into declassified region. Narrow band of misclassified pixels indicated by yellow arrow in (a) is removed in (c).

equalized to prevent biased segmentation results due to leakage of the DC component through the filters [4]-[6].

The results in Fig. 5 illustrate the effects of the proposed method on misclassifications at texture boundaries. The image in Fig. 5(a) consists of an outermost region of Gaussian-distributed lowpass noise, a middle ring of "French canvas", and an innermost square region of "straw matting" from the Brodatz album [7].

Fig. 5(b) is the classifier output c(x,y) without the proposed method. A prominent band of misclassified pixels is seen along the entire boundary between the outermost texture (noise) and the middle ring of texture (French canvas). Applying the proposed operator to Fig. 5(b) results in the final segmented image $i_S(x,y)$ in Fig. 5(c). Comparing Fig. 5(b) and (c), the pixels misclassified as a third texture at the texture boundary are removed by the proposed methods.

5. Conclusion

An N-ary morphological operator is presented for the removal of narrow bands of misclassified pixels near boundaries. The first step of the proposed operator resembles an N-ary erosion, where pixels in certain inhomogeneous regions are temporarily declassified. The second step resembles an N-ary dilation as regions grow to fill in the temporarily declassified regions from the first step.

In addition, a one-dimensional example is used to illustrate the inevitability of transient misclassifications at region boundaries. The transients arise as a consequence of the bandwidth of a filtering process, as is commonly used to generate feature vectors. An example is given where the transient response of the filter must pass through regions of feature space causing erroneous classification. As a filtered image makes a transition between the mean amplitudes of two classes comprising a boundary, the feature amplitude may have to pass through an intermediate amplitude level erroneously assigned to a third class.

6. References

[1] A. K. Jain, F. Farrokhnia, "Unsupervised texture segmentation using Gabor Filters," Pattern Recognition, pp. 1167-1186, 1991.

[2] M. Unser, "Texture Classification and Segmentation Using Wavelet Frames," IEEE Trans. Image Proc., pp. 1549-1560, 1995.

[3] C.S. Lu, P.C. Chung, C.F. Chen, "Unsupervised texture segmentation via wavelet transform," Pattern Rec., pp. 729-742, 1992.

[4] T. P. Weldon and W. E. Higgins, "Designing Multiple Gabor Filters for Multi-Texture Image Segmentation," *Optical Engineering* , Vol. 38 No. 9 , pp. 1478-1489 , Sept. 1999.

[5] T. P. Weldon, W. E. Higgins, and D. F. Dunn, "Efficient Gabor Filter Design for Texture Segmentation," *Pattern Recognition* , Vol. 29, No. 12, pp. 2005-2015, Dec. 1996.

[6] T. P. Weldon, W. E. Higgins, and D. F. Dunn, "Gabor Filter Design for Multiple Texture Segmentation," *Optical Engineering*, Vol. 35 No. 10, pp. 2852-2863, October 1996.

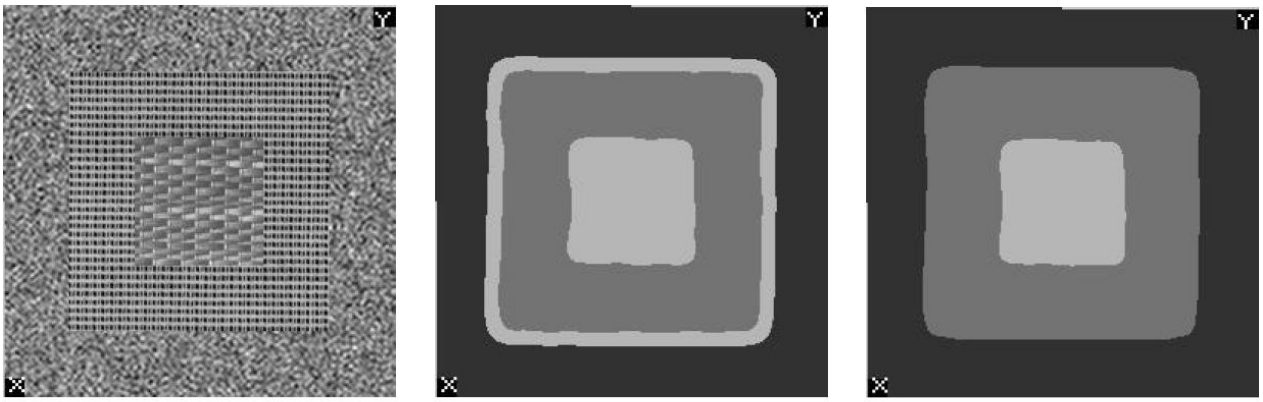

(a) (b) (c)

Figure 5. Effect of proposed post-processing. (a) Input composite image, outer border of Gaussian noise, middle ring of "french canvas," center square of "straw matting." (b) Output of classifier without post-processing showing a narrow ring misclassified as the center texture at the boundary between the two outermost textured regions. (c) Final segmentation after post-processing to remove misclassification at texture boundaries, measured segmentation error = 0.05.

[7] P. Brodatz, *Textures: A Photographic Album for Artists and Designers*. New York, NY: Dover, 1966.

[8] T. P. Weldon, "Improved Image Segmentation with a Modified Bayesian Classifier," *IEEE Transactions on Acoustics, Speech, and Signal Processing,* May 2006.

[9] Anil K. Jain, *Fundamentals of Digital Image Processing*, Englewood Cliffs, NJ, Prentice Hall, 1989.

[10] Raphael C. Gonzalez and Richard E. Woods, *Digital Image Processing*, Upper Saddle River, NJ, Prentice Hall, 2002.